Chiral Phosphite Mediated Photoredox Catalyzed Aerobic Oxidative DYKAT for C–N Atropoisomers

Pinku Saikia, Ayantika Bhattacharjya,[§] Susmita Maity,[§] Priyam Bajpai,[§] M Aarthika,[§] Asish Bera, Arindam Saha, Rajesh G. Gonnade, Kumar Vanka, and Pradip Maity*

ABSTRACT: Atroposelective compounds with axial chirality are important structural motifs in medicinal chemistry and materials science. Among these, anilides with a chiral C(=O)–N axis are intriguing structural motifs with several applications. Traditionally, the synthesis of these compounds has relied on the direct installation of the chiral C(sp^2)–N(sp^2) bond or enantioselective modification to the peripheral groups to increase steric around the C–N axis. However, these methods are limited in substrate scope and are constrained by the type and size of functional groups compatible with these strategies. Here, we show that phosphite-enabled loss of planarity led to a Dynamic Kinetic Asymmetric Transformation (DYKAT) for the oxidation of iminium ions to access enantioenriched isoquinolones. This method expands the substrate scope, tolerating a wide variety of positional, steric, and electronic substitution patterns that were previously challenging or inaccessible. Furthermore, the phosphite-mediated approach is versatile, facilitating the synthesis of atroposelective pyridone, lactam, and acyclic anilide. These results demonstrate a conceptually new strategy for atroposelective synthesis that complements traditional methods in terms of substrate diversity. Computational studies support the phosphite mediated change in hybridization for DYKAT prior to the oxidation step, paving the way for future studies in the synthesis of complex axially chiral molecules.

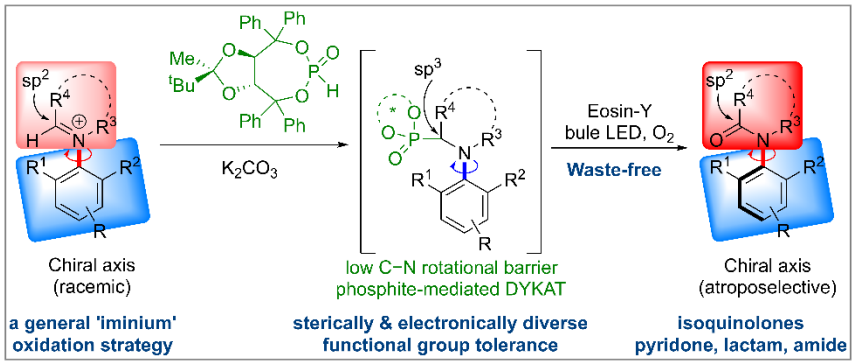

Atropoisomers with chiral C(sp^2)–N(sp^2) bonds became a synthetic focus due to their occurrence in natural products and synthetic drugs, bioactive molecules, chiral ligands, organocatalysts, and smart materials.[1] Among them, anilides are an important class,[2] and the atropoisomerism around those led to new class of synthetic drugs with increased selectivity (Figure 1).[3] Controllable rotations around the atropoisomeric bonds are one of the approaches to building molecular rotors and motors.[4] Owing to their importance and potential, an intense focus on their synthesis, and in general atroposelective synthesis, is underway.[5] The substrate scope to install atroposelective C–N bond formation is generally limited, likely due to the sterically sensitive activation modes.[6] The peripheral modification around an N-aryl bond for atroposelectivity can be classified into four main categories: i) *de novo* N-pyridone or aromatic ring formation,[7] ii) asymmetric N–H functionalization,[8] iii) asymmetric C–H functionalization around pyridone/anilides,[9] and iv) desymmetrization (Figure 2).[10] Most of these reported methods rely on transition metal catalysis that requires suitably pre-functionalized starting materials. As a result, the substitution pattern and substrate scope are dependent on the reaction type and catalyst system, leading to products with specific functional groups. Organocatalysis, such as chiral phosphoric acid and NHC catalysts, was also reported via cyclization–condensation methods with specific functional group requirements.[7c,f,8c,i,j] Therefore, despite the recent focus and progress, synthesis of atroposelective pyridones and anilides with a wide range of substitution pattern remains a fundamental challenge.

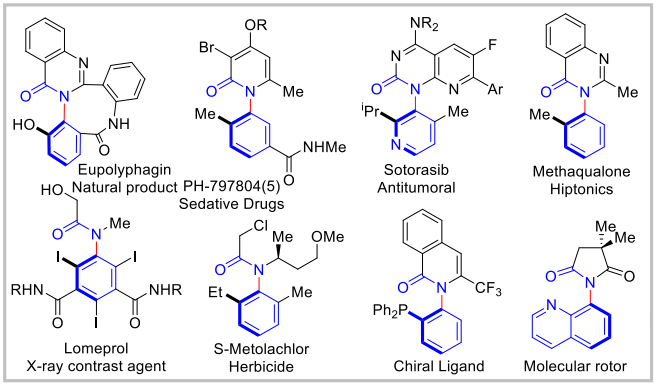

Figure 1. Representative atroposelective compounds with chiral C(=O)–N axis

https://doi.org/10.26434/chemrxiv-2025-1l3kn **ORCID:** https://orcid.org/0000-0001-8493-3171

Our research focus on chiral phosphite catalyzed asymmetric functionalization of azaarenium salts presents us with a possibility to obtain axially chiral C−N bond formation via a new route. We anticipated that the oxidation of the phosphite adduct of iminium ion could lead to the anilide formation with phosphite controlled atroposelectivity (Figure 2F).[11] Herein, we report a chiral phosphite and photoredox catalyzed aerobic oxidation of N-aryl isoquinolinium salts to atroposelective isoquinolones via DYKAT. Our protocol is notable for its success without the need for an auxiliary group, leading to wide variety of substituents at all positions on both N-aryl group and isoquinoline. Experimental and computation studies were conducted to understand the mechanism and the source of stereoinduction. The requirement of only C=N for its oxidation is demonstrated by extending our method for the oxidation of cyclic and acyclic iminium substrates to lactum and anilides respectively. A pyridinium substrate was also successfully oxidized to atroposelective pyridone. The chiral influence of atropoiosmeric N-aryl groups on isoquinolone products was utilized to functionalize the enamide bond diastereoselectively.

We started with the synthesis of isoquinolinium salt **1** from the corresponding Zincke salt and aniline derivative.[12] The salt **1** is also expected to have a restricted rotation around C−N depending on the steric around it. In fact, N-aryl isoquinolinium and dihydroisoquinolinium natural products such as ancisheynine and ancistrocladiniums are known atropoisomers.[13] Since the size of oxygen in product **6** is bigger than hydrogen in starting salt **1**, a dynamic kinetic resolution (DKR) is feasible with sterically tailored functional groups, while a bigger steric would lead to kinetic resolution (KR). However, we hypothesize that our proposed phosphite catalyst adduct **2**, with a change in the hybridization of iminium carbon from sp2 to sp3, could lower the C−N rotational barrier. In that scenario, a chiral phosphite-mediated dynamic kinetic asymmetric transformation (DYKAT) could be achieved with sterically bulky substituents as well.[14]

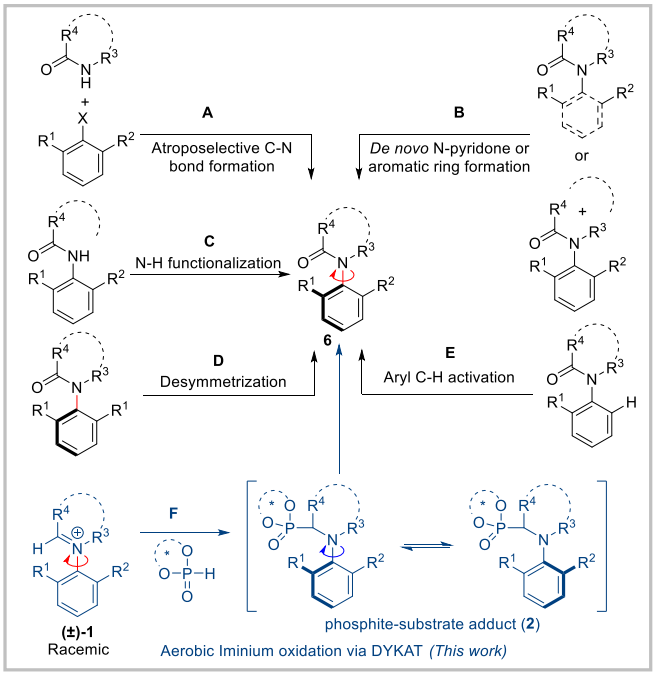

Figure 2. Strategies for atrposelective synthesis of anilides.

To test this hypothesis, we calculated the C−N bond rotational energies computationally for two starting materials and their phosphite adducts with chiral phosphite **P1**. The computationally determined rotational energy decreased significantly for the catalyst adducts (**2**) by 6.0-12.1 kcal/mol (Scheme 4b; see SI for details). ^{1}H NMR of **2a** recorded in $CDCl_3$ at room temperature shows only two diastereomers due to the formation of a new chiral center at C1 carbon. No extra diastereomers were detected for the restricted C−N bond rotation. Therefore, we anticipated that the faster C−N bond rotation in intermediate **2** compared to its oxidation rate would allow atroposelective product (**6**) formation via DYKAT (Figure 2F).

With a feasible phosphite-mediated DYKAT, we next focused on the oxidation to isoquinolone (**6a**) synthesis. A mild and waste-free aerobic oxidation under photoredox conditions would be ideal for sustainability.[11,15] Hence, we started with a dual catalysis approach with 20 mol% chiral phosphite catalyst **P1** and Eosin Y as the photocatalysts under blue light irradiation in an oxygen atmosphere. Subjecting **1a** to the above reaction condition successfully led to the complete consumption of the starting material to 58% product (**6a**) formation, however, with only a 58:42 enantiomeric ratio (Table 1, entry 1).

Table 1: Reaction Optimization Study

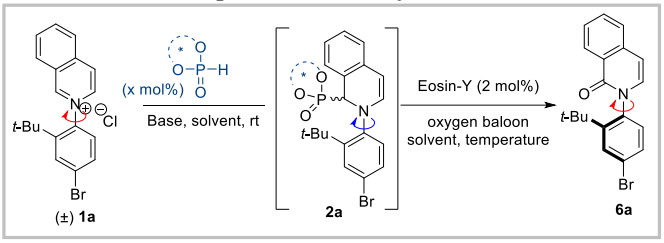

entry	Phosphite	Solvent	T (°C)	Yield (%)	er
1[a]	P1	THF	0	58	58:42
2	-	THF	0	65	-
3	P1	THF	0	83	83:17
4[b]	P1	THF	0	80	75:25
5[b]	P1	THF	0	83	87:13
6	P1	THF	0	83	91:9
7	P1	diff. solvents	0	63-83	<91:9
8	P1	THF	-5	83	92:8
9	P1	THF	-10	78	91:9
10	P2	THF	-5	36	93:7
11	P10	THF	-5	80	91:9
12	P11	THF	-5	81	96:4
13[c]	P11	THF	-5	<5	-
14[d]	P11	THF	-5	<5	-
15[e]	P11	THF	-5	80	96:4

Otherwise mentioned all reactions were carried out at 0.1 mmol scale with 2 ml of solvent, stoichiometric phosphite, 2 mol% Eosin-Y, 50 W blue LED light, and under an oxygen atmosphere. [a]20 mol% P1, [b]35 mol% P1. [c]In the absence of light. [d]In the absence of photocatalyst. [e] Reaction with recovered phosphite catalyst.

A background reaction check without the phosphite catalyst reveals an alternative light-mediated racemic oxidation path (entry 2).[16] To avoid background reaction, stoichiometric phosphite was taken next to fully convert the starting material to the adduct (**2a**) before its photocatalytic oxidation, which led to an 83% yield and an encouraging 83:17 enantiomeric ratio (entry 3). For a sub-stoichiometric catalytic path, the substrate was added portion-wise to prevent its presence during the subsequent photocatalytic oxidation. Substrate addition in three repeated cycles with 35 mol% phosphite catalyst **P1** resulted in a comparable yield, but with lower enantioselectivity than that of the stoichiometric one (entry 4 *vs*. 3). Screening of base and counter anion of the starting material showed that the enantioselectivity is sensitive and diminishes in their presence (see SI). Although the optimal choice of counter anion, base, and its addition sequence improved the enantiomeric ratio to 87:13 (entry 5), the oxidation of adduct **2a** free from those ionic entities led to a higher enantiomeric ratio (entry 6). Therefore, we opted for a stoichiometric phosphite-mediated adduct formation followed by its photoredox aerobic oxidation after quick filtration. The phosphite catalyst was recovered via column chromatography during the product purification and reused. A quick solvent screening revealed that THF remained the best one (entry 7). The screening of temperature led to the best result at -5 °C with a slightly improved enantiomeric ratio (entry 8). With optimal reaction conditions in hand, we screened various phosphite catalysts by modifying the aryl and diol-protecting groups of the chiral TADDOL backbone. Replacing the phenyl group with 2-methylphenyl (**P2**) led to an increase in enantioselectivity, but the yield dropped to 36% (entry 10). Other electronically and sterically different aryl groups tested did not improve the outcome (see SI for complete phosphite screening). Next, we varied the diol protecting group on TADDOL. Protection with an unsymmetrical methyl, *tert*-butyl ketone (**P11**) led to maximum enantiomeric ratio of 96:4 (entry 12). The presence of light and photocatalyst is essential for the reaction (entries 13-14). The recovered phosphite was tested for its recyclability that resulted in identical result (entry 15).

The optimization of the reaction condition prompts us to test the generality of our aerobic oxidative method (Figure 3). First, we screened electronically diverse functional groups on the N-aryl ring, keeping the bulky *ortho*-*tert*-butyl substituent to attain atroposelectivity. An unsubstituted aryl ring did not affect the reaction outcome. An iodo in para-position worked well (**6b**), while chloro-substitution led to a slightly diminished yield and enantiomeric ratio (91:9) (**6c**). For other *para*-substitution, an electron-donating benzyloxy group was well tolerated (**6e**), while the enantiomeric ratio decreased to 86:14 er for electron-withdrawing cyano substitution (**6f**). Different aryl substitutions, such as phenyl, 2-benzofuran, and 2-benzothiophene, led to good yields while maintaining very good enantiomeric ratios (**6g-i**). An alkene substitution resulted in good yield and enantiomeric ratio, but the E-stilbene was converted to a major Z diastereomer in the product (**6j**) via photoisomerization.[17] Substitutions at other positions such as *meta* (**6k-l**) and *meta*, *para* double substitutions (**6m**) were uneventful with good yields, while the enantioselectivity drops slightly for the electron-withdrawing nitro group at the *meta* position (**6l**). Next, we examined substrates with 2,6-disubstituted aryl rings to find the feasibility of DYKAT with increased steric around C−N. 2-Bromo-6-methyl substituted substrates underwent complete conversion to form the products **6n** and **6o** in >80% yield and 87.5:12.5 enantiomeric ratio. The high yield and enantiomeric ratio confirmed successful DYKAT over simple kinetic resolution (KR). To further test the steric difference as the stereo-controlling factor, we subjected 2-bromo-6-ethyl substrate under the optimized reaction condition. Expectedly, the enantiomeric ratio decreased to 76.5:23.5 while the yield remained unaffected (**6p**). 2-Chloro-6-methyl and 2-fluoro-6-methyl substitutions also led to successful DYKAT. As the size of the halogen decreases, enantioselectivity gradually diminishes, resulting in an enantiomeric ratio of 81:19 for chloro (**6q**) and 77.5:22.5 for fluoro (**6r**). The diminished steric differences between the two *ortho* substituents presumably determine the enantioselectivity trend.[18] Encouraged by the success of a variety of groups on both the *ortho* positions to exert enantioselectivity, we tested other combinations to find out their effectiveness. Dihalo substitutions such as bromo and fluoro led to 60:40 enantiomeric ratio (**6s**), while chloro and fluoro gave a poor 54:46 enantiomeric ratio (**6t**). With methoxy and fluoro, the enantiomeric ratio remained poor as well (**6u**). In all cases, the reaction remained efficient with good yields.

After achieving a broad functional group tolerance on the N-aryl ring, we focused on the isoquinoline derivatives next. We started with substitution on the fused benzene ring of the isoquinoline. Methoxy, phenyl, and bromo all worked well at C5 with good yields and enantioselectivity (**6v-x**). Those same substitutions at the C6 position also led to good yields and enantioselectivities (**6y-z**, **6aa**). Bromo substitution at C7 was equally efficient (**6ab**). We could not synthesize C8 substituted substrates to test their compatibility. However, the isoquinolone oxygen in the product is known to act as a coordinating group to functionalize C8 hydrogen via transition metal catalysis to obtain C8 functionalized atroposelective isoquinolone.[7k] Finally, we tried substitutions on the azaarene ring carbons. Both phenyl and bromo substituted substrates on C4 carbon were successful, albeit with lower enantiomeric ratios (**6ac-ad**). The synthesis of C3 substituted starting materials was unsuccessful via its Zincke salt, but we synthesized the C3 phenyl starting material via a different literature-reported approach.[19] Our oxidation method successfully formed the corresponding product with moderate yield a low enantiomeric ratio of 69:31, probably due to the smaller steric differences in the two *ortho* positions with methyl and hydrogen (**6ae**). Overall, our aerobic oxidative method that does not require any auxiliary functional group led us to synthesize atroposelective isoquinolones with substitutions at each position. The mild nature of the catalytic method allows a broad variety of functional group tolerance. The enantioselectivity trends with a variety of sterically different substitutions provide an insight into the probable combinations to achieve good selectivity.

To gain insight into our new aerobic oxidative approach and to find the stereo-defining step for DYKAT, we conduct extensive experimental and theoretical studies. Since a diastereomeric phosphite catalyst adduct (**2**) formed via the generation of a new chiral center, we tested its potential effect on product stereochemistry. The adduct formation at different temperatures led to different diastereomeric ratios (dr) with poor dr, but all those resulted in the formation of product in same enantiomeric ratio at optimal aerobic oxidation temperature.[20] On the other hand, starting with a defined diastereomeric ratio of 1:0.85 led to product with different enantiomeric ratios when the subsequent photoredox oxidation step was carried out at different temperatures (Figure 4A).

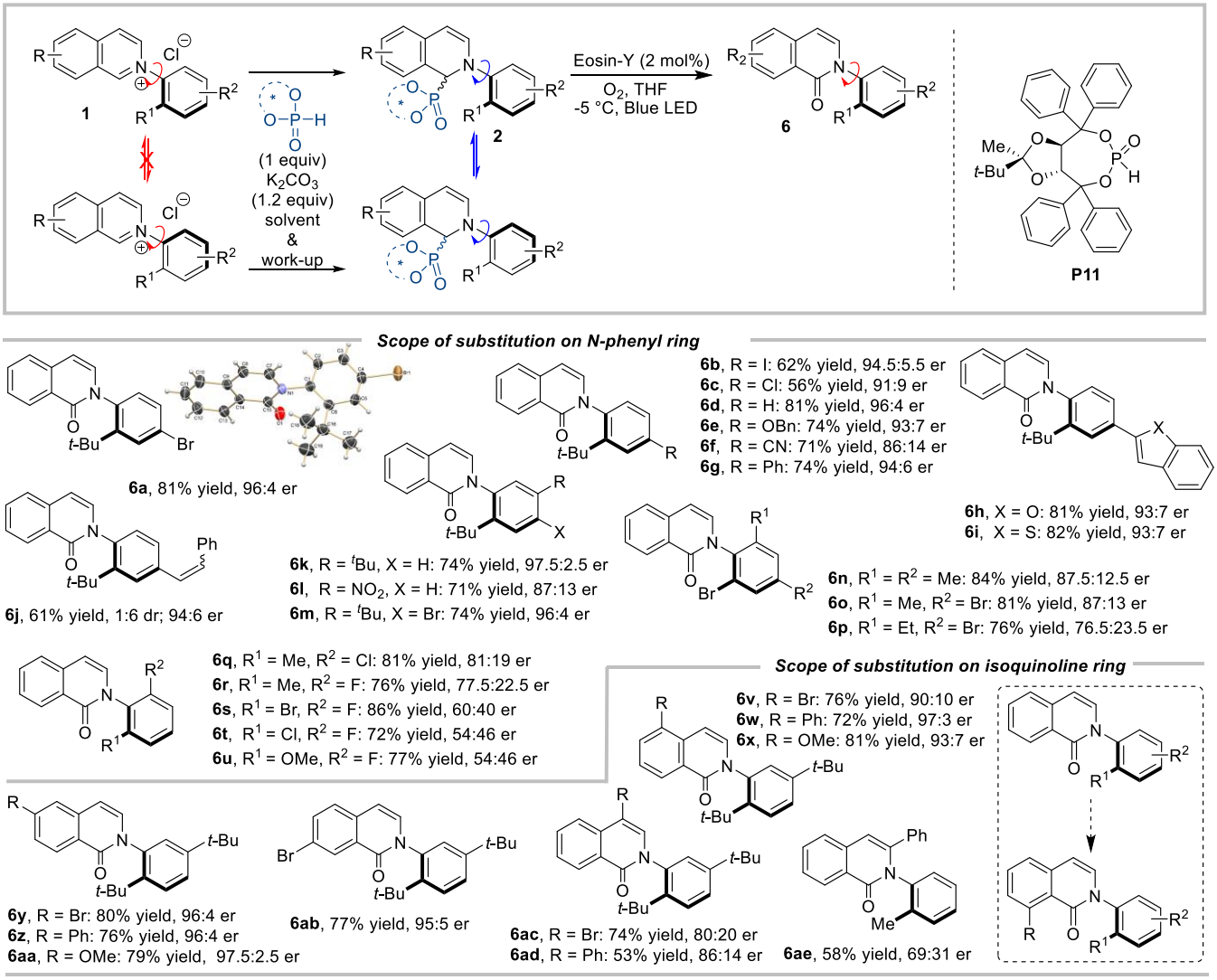

Figure 3. Substrate scope. All reactions were performed on a 0.1 mmol scale.

These results establish that the selectiv formation of central chirality in intermediate **2** is inconsequential, and the chiral phosphite controlled stereo-differentiation occurs during the re-generation of the planner chirality (Figure 4A).

The oxidation process starts via single-electron oxidation of the nitrogen of intermediate **2** by eosin Y under light irradiation. The oxidation potential of **2a** is determined to be 0.59 V; lower than that of the photocatalyst. The reduced photocatalyst is oxidized back by oxygen with the formation of superoxide radical.[16a,21] A deprotonation of highly acidic α-H would lead to the formation of the corresponding α-carbon radical **3** (*path A*, Figure 4C), while hydrogen atom abstraction (HAT) by superoxide radical would directly generate isoquinolinium intermediate **4** and hydroperoxide anion (*path B*, Figure 4C).[21] The α-amino carbon radical **3** could either undergo a single electron transfer with peroxy radical to form **4** and hydroperoxide anion, or form product via C–O bond formation with peroxy radical.[11a,17] The intermediacy of **4** results in the formation of hydrogen peroxide, and requires water to form the final product via an addition-elimination mechanism (Figure 4C). To distinguish between the reactions paths operating here, we conducted the photoredox step in the presence of $^{18}O_2$ and H_2O^{18} separately. The presence of labeled oxygen did not incorporate it into the product while labeled water led to the product with major ^{18}O incorporation (Figure 4D).[16,17] Conducting the reaction in the presence of a drying agent led to significant reduction in the product formation (36%) and the detection of intermediates **4** and **5** by HRMS (Figure 4E). The presence of peroxide was also detected via GC-MS analysis of crude reaction mixture. On the other hand, adduct of intermediate **3** with peroxy radical was not detected.[17] The recovery and recycling of phosphite catalyst suggests its oxidative stability under peroxide, which we demonstrated separately (see SI).

To understand the DYKAT[21] process and stereo-determining step, we turned our attention to the C–N bond rotation and reaction parameters that influence the enantiomeric ratio. First, a minimum energy calculation and the C–N bond rotational energy analysis were done computationally for the starting materials (**1**), products (**6**), and proposed intermediates (**2** & **5**) (Figure 4A & 4G; see SI for detailed analysis). The calculations were done at the PBE[15a]/D3[15b]-TZVP[15c] level of theory, with Turbomole 7.5.[15d] The calculated rotational barriers of mono- and di-*ortho* substituted starting materials (**1a** & **1o**) and products (**6a** & **6o**) indicate that those exibit atropoisomerism.

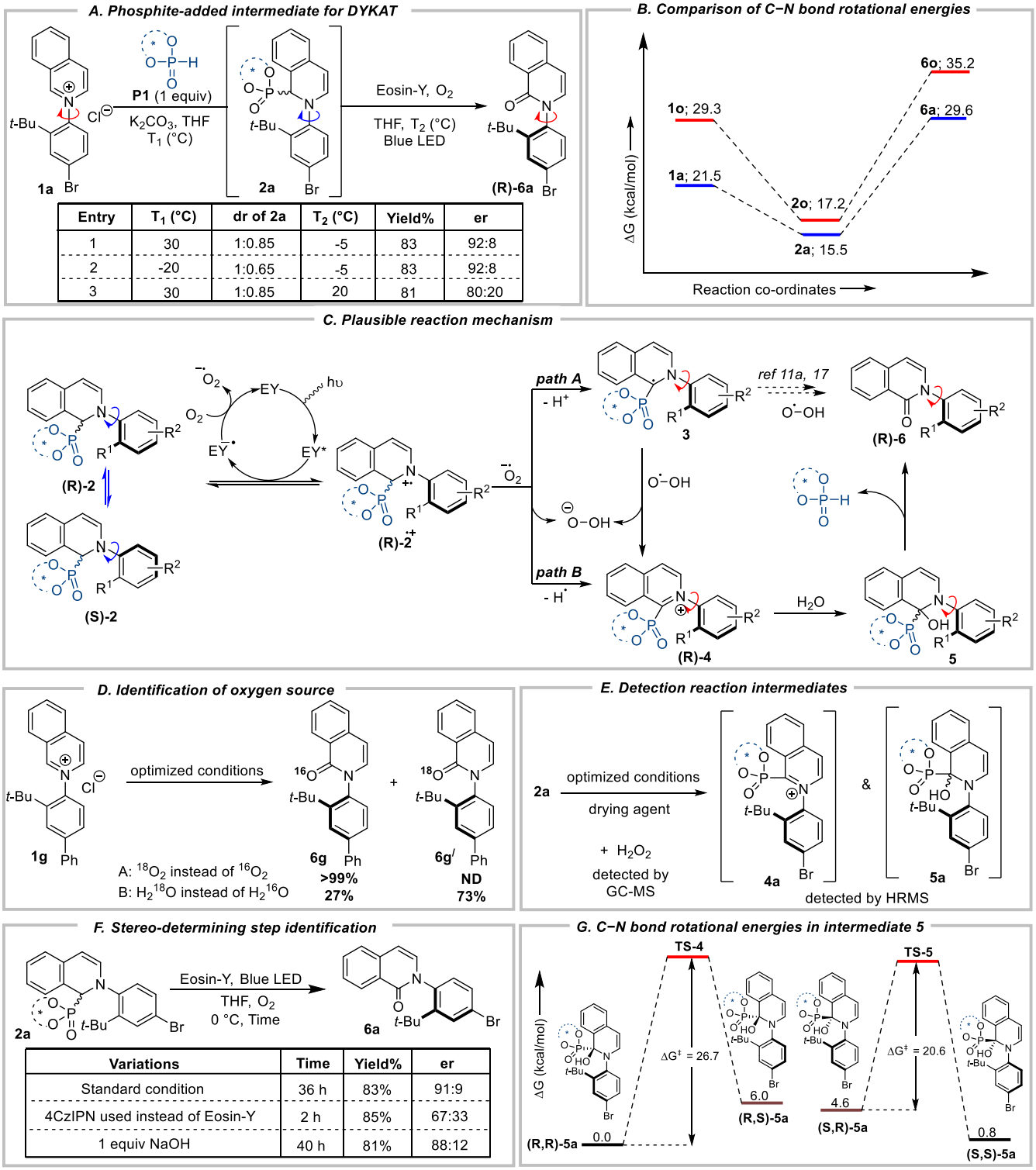

Entry	T_1 (°C)	dr of 2a	T_2 (°C)	Yield%	er
1	30	1:0.85	-5	83	92:8
2	-20	1:0.65	-5	83	92:8
3	30	1:0.85	20	81	80:20

Variations	Time	Yield%	er
Standard condition	36 h	83%	91:9
4CzIPN used instead of Eosin-Y	2 h	85%	67:33
1 equiv NaOH	40 h	81%	88:12

Figure 4. Mechanistic investigation.

Experimentally determined C–N bond rotational energy in **6a** closely matches with the computational value (see SI for details), validating the computational method. The product stereochemistry of C–N atropoisomer is (R), determined by single crystal structure of **6a** (Figure 3). Therefore, rotation of diastereomeric intermediates of **2** with (S) conformation around C–N are relevant to achieve DYKAT. For **2a**, those rotational energies are 12.8 and 15.5 kcla/mol, while in **2o**, the corresponding energies are 18.0 and 17.2 kcal/mol. The computational C–N bond rotational frequencies and half-lives for racemization are in seconds for these intermediate (**2**) (see SI). For the other intermediate with sp^3 α-carbon (**5**), the rotational energies are 20.6 and 26.7 kcla/mol with half-lives for racemization are in hours to years. The DYKAT achieved experimentally

suggests the stereo-differentiating step is slower than the racemization. To gain experimental insight, we tweaked the photoredox aerobic oxidation procedure to observe the effect in DYKAT. 4CzIPN as photoredox catalyst with a stronger oxidation potential than Eosin-Y led to significantly faster reaction, but with considerably lower enantiomeric ratio (Figure 4F). This result suggests that the DYKAT occurs during the photoredox oxidation of **2** to **4**. The addition of hydroxide is expected to enhance the rate of formation of **6** from **4**. But it did not enhance the overall oxidation process or reduce the enantioselectivity, further supporting oxidation of **2** as the rate- and enantio-determining step.

Synthetic modifications of the atroposelective isoquinolones and their utilities were well documented in recent literature.[6-10] Here, we plan to take advantage of the chiral C−N bond for diastereoselective functionalization of the adjacent C=C in isoquinolone.[23] Cyclobutanes are frequently encountered in natural products and pharmaceuticals, and a photochemical [2+2] cycloaddition remains the simplest and most utilized path to the four-membered ring formations.[24] However, the stepwise radical mechanism poses challenges for their regio- and stereoselective synthesis. Only a few asymmetric approaches have emerged recently for chiral cyclobutane synthesis.[25] We treated chiral **6e** with electron deficient alkene coupling partner acrylonitrile, which led to the formation of [2+2] product **7** in a regio- and stereoselective fashion (Figure 5A). The major diastereomer was isolated in 73% yield and the stereochemistry was determined via comparing its NMR spectral data with the reported literature.[25b,26] The selective generation of three new chiral centers in and around dihydroisoquinolone is significant as it is a structural feature present in many biologically active alkaloids.[27] Next, we treated substrate **6ae** with phenyl-substituted enamide for its hydrogenation via Pd/C catalyst, which led to the formation of inseparable diastereomers of dihydroisoquinolones **8** in 4:1 ratio. The steric bulk of methyl versus hydrogen is not as drastic as it is with other bigger groups such as a *tert*-butyl. Screening of sterically or electronically different groups along with optimization of hydrogenation method could lead to better selectivity.[28]

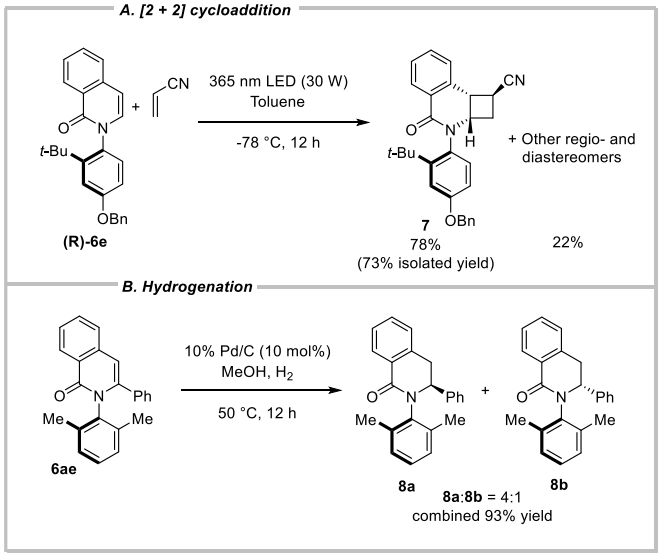

Figure 5. Product derivatization via diastereoselective functionalization of enamide.

Our aerobic oxidation of 'iminium' embedded in isoquinoline without any auxiliary functional group requirement allows us to synthesize isoquinolone with a wide variety of positional and functional substitutions. This success led us to question whether the 'iminium' has to be a part of azaarene for its oxidation or not. To test the generality of 'iminium' oxidation via our protocol, we screened non-aromatic cyclic and acyclic iminium salts **9** and **12**. We were delighted to obtain the corresponding lactam **11** and anilide **14** under our reaction condition with 45% & 22% yields and 84:16 & 72.5:27.5 enantiomeric ratios (Scheme 6A and 6B). These results are remarkable, and they pave the way to a general synthetic approach for atroposelective anilides.

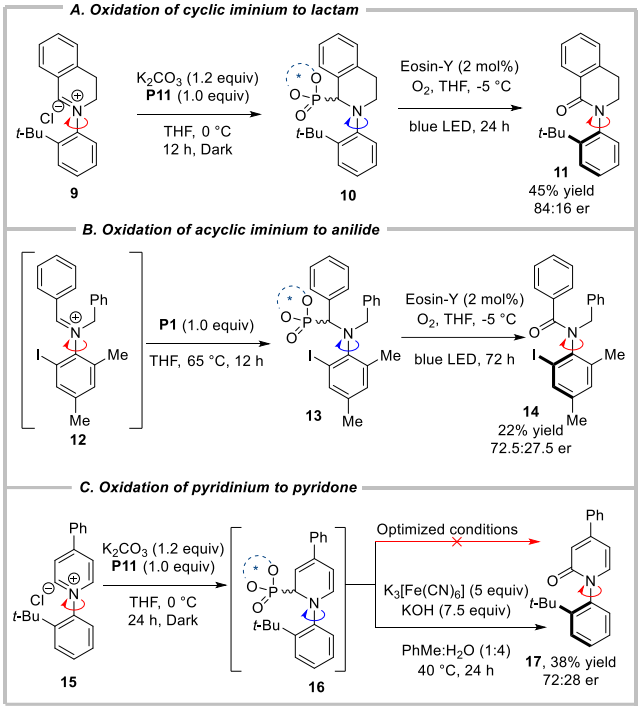

Figure 6. Extension of phosphite catalyzed oxidative DYKAT with other 'iminium' substrates.

For 4-phenyl pyridone, the phosphite catalyst adduct from the pyridinium formed successfully, while the subsequent photocatalytic aerobic oxidation did not occur. Subsequently, we tested other photocatalysts and oxidants to oxidize the intermediate **16**. Although other aerobic photocatalytic methods screened did not give satisfactory results, we found that a chemical oxidant potassium ferricyanide oxidized the intermediate with a moderate 38% yield and 72:28 enantiomeric ratio (Figure 6C).[29] These results suggest that reoptimization of reaction parameters and chiral phosphite catalyst is necessary to use our protocol for other anilide syntheses.

In conclusion, we developed a chiral phosphite-mediated oxidative DYKAT of iminium for the synthesis of atroposelective anilides with a chiral C−N bond. For iminium embedded in isoquinoline, a dual phosphite and aerobic photoredox catalytic was successful in synthesizing N-aryl isoquinolone. Since no other functional group was required for this mild aerobic oxidation, a broad range of substituents were tolerated at different positions on either aromatic ring. Experimental and computational studies established plausible reaction mechanism and

origin for phosphite catalyzed DYKAT. The atroposelective C–N bond was utilized to functionalize isoiquinolone to chiral dihydroisoquinolone derivatives. The chiral phosphite-catalyzed DYKAT method was extended to pyridine-embedded iminium as well as non-heteroaromatic cyclic and acyclic iminium ions. Currently, we focus on establishing a phosphite-catalyzed atroposelective method for iminium ion functionalization.

ASSOCIATED CONTENT

Supporting Information

The Supporting Information is available free of charge at

AUTHOR INFORMATION

Corresponding Author

Pradip Maity – *Organic Chemistry Division, CSIR-National Chemical Laboratory, Pune-411008, India; Academy of Scientific and Innovative Research (AcSIR), Ghaziabad 201002, India; orcid.org/0000-0001-8493-3171*; Email: p.maity@ncl.res.in

Authors

Pinku Saikia – *Organic Chemistry Division, CSIR-National Chemical Laboratory, Pune-411008, India; Academy of Scientific and Innovative Research (AcSIR), Ghaziabad 201002, India*

Ayantika Bhattacharjya – *Organic Chemistry Division, CSIR-National Chemical Laboratory, Pune-411008, India; Academy of Scientific and Innovative Research (AcSIR), Ghaziabad 201002, India*

Susmita Maity – *Organic Chemistry Division, CSIR-National Chemical Laboratory, Pune-411008, India; Academy of Scientific and Innovative Research (AcSIR), Ghaziabad 201002, India*

Priyam Bajpai – *Physical and Material Chemistry Division, CSIR-National Chemical Laboratory, Pune-411008, India; Academy of Scientific and Innovative Research (AcSIR), Ghaziabad 201002, India*

M Aarthika – *Organic Chemistry Division, CSIR-National Chemical Laboratory, Pune-411008, India; Academy of Scientific and Innovative Research (AcSIR), Ghaziabad 201002, India*

Asish Bera – *Organic Chemistry Division, CSIR-National Chemical Laboratory, Pune-411008, India; Academy of Scientific and Innovative Research (AcSIR), Ghaziabad 201002, India; orcid.org/0000-0001-262 7301-7573*

Arindam Saha – *Catalysis and Inorganic Chemistry Division, CSIR-National Chemical Laboratory, Pune-411008, India; Academy of Scientific and Innovative Research (AcSIR), Ghaziabad 201002, India; orcid.org/ 0000-0002-0421-0633*

Rajesh G. Gonnade − *Physical and Materials ChemistryDivision, CSIR-National Chemical Laboratory, Pune411008, India; Academy of Scientific and InnovativeResearch (AcSIR), Ghaziabad 201002, India; orcid.org/ 0000-0002-2841-0197*

Kumar Vanka – Physical and Material Chemistry Division, *CSIR-National Chemical Laboratory, Pune-411008, India; Academy of Scientific and Innovative Research (AcSIR), Ghaziabad 201002, India*

Complete contact information is available at:

Author Contributions

§M. A., A.B., P.B., and S. M. contributed equally to this work.

Notes

The authors declare no competing financial interest.

ACKNOWLEDGMENT

This research was supported by the SERB (SCP/2022/000465). P.S. thank CSIR, M. A. and P.B. thank INSPIRE for a fellowship. The support from central analytical facility, NCL is greatly acknowledged. The support and the resources provided by 'PARAM Brahma Facility' under the National Supercomputing Mission, Government of India at the Indian Institute of Science Education and Research (IISER) Pune are gratefully acknowledged.

REFERENCES

(1) (a) Kumarasamy, E., Raghunathan, R., Sibi, M. P. & Sivaguru, J. Nonbiaryl and heterobiaryl atropisomers: molecular templates with promise for atropselective chemical transformations. *Chem. Rev*. **2015**, *115* (20), 11239–11300. (b) Wu, Y.-J.; Liao, G.; Shi, B.-F. Stereoselective Construction of Atropisomers Featuring a C–N Chiral Axis. *Green Synth. Catal*. **2022**, *3* (2), 117–136. (c) Xiao, X.; Chen, B.; Yao, Y.-P.; Zhou, H.-J.; Wang, X.; Wang, N.-Z.; Chen, F.-E. Construction of Non-Biaryl Atropisomeric Amide Scaffolds Bearing a C-N Axis via Enantioselective Catalysis. *Molecules* **2022**, *27* (19), 6583. (d) Roos, C. B.; Chiang, C.-H.; Murray, L. A. M.; Yang, D.; Schulert, L.; Narayan, A. R. H. Stereodynamic Strategies to Induce and Enrich Chirality of Atropisomers at a Late Stage. *Chem. Rev*. **2023**, *123* (17), 10641–10727. (e) Basilaia, M.; Chen, M. H.; Secka, J.; Gustafson, J. L. Atropisomerism in the Pharmaceutically Relevant Realm. *Acc. Chem. Res*. **2022**, *55* (20), 2904–2919. (f) Kitagawa, O. Chiral Pd-Catalyzed Enantioselective Syntheses of Various N-C Axially Chiral Compounds and Their Synthetic Applications. *Acc. Chem. Res*. **2021**, *54* (3), 719–730.

(2) (a) Jiang, H.-L.; Luo, X.-H.; Wang, X.-Z.; Yang, J.-L.; Yao, X.-J.; Crews, P.; Valeriote, F. A.; Wu, Q.-X. New Isocoumarins and Alkaloid from Chinese Insect Medicine, Eupolyphaga Sinensis Walker. *Fitoterapia* **2012**, *83* (7), 1275–1280. (b) Guan, C.-Y.; Zou, S.; Luo, C.; Li, Z.-Y.; Huang, M.; Huang, L.; Xiao, X.; Wei, D.; Wang, M.-C.; Mei, G.-J. Catalytic Asymmetric Synthesis of Planar-Chiral Dianthranilides via (Dynamic) Kinetic Resolution. *Nat. Commun*. **2024**, *15* (1), 4580. (c) Xing, L.; Devadas, B.; Devraj, R. V.; Selness, S. R.; Shieh, H.; Walker, J. K.; Mao, M.; Messing, D.; Samas, B.; Yang, J. Z.; Anderson, G. D.; Webb, E. G.; Monahan, J. B. Discovery and Characterization of Atropisomer PH-797804, a P38 MAP Kinase Inhibitor, as a Clinical Drug Candidate. *ChemMedChem* **2012**, *7* (2), 273–280. (d) Kargbo, R. B. Improved Synthesis of New FDA-Approved Treatment for KRAS G12C Mutation in Non-Small Cell Lung Cancer. *ACS Med. Chem. Lett*. **2021**, *12* (8), 1186–1187. (e) Inger, J. A.; Mihan, E. R.; Kolli, J. U.; Lindsley, C. W.; Bender, A. M. DARK Classics in Chemical Neuroscience: Methaqualone. *ACS Chem. Neurosci*. **2023**, *14* (3), 340–350. (f) Anelli, P. L.; Brocchetta, M.; Lattuada, L.; Uggeri, F. Green Approaches to the Production of Iopamidol. *Pure Appl. Chem*. **2011**, *84* (3), 485–491. (g) Yang, P.; Wang, X.; Peng, L.; Chen, F.; Tian, F.; Tang, C.-Z.; Wang, L.-X. Optimized Synthetic Route for Enantioselective Preparation of (S)-Metolachlor from Commercially Available (R)-Propylene Oxide. *Org. Process Res. Dev*. **2017**, *21* (10), 1682–1688.

(3) (a) Canon, J.; Rex, K.; Saiki, A. Y.; Mohr, C.; Cooke, K.; Bagal, D.; Gaida, K.; Holt, T.; Knutson, C. G.; Koppada, N.; Lanman, B. A.; Werner, J.; Rapaport, A. S.; San Miguel, T.; Ortiz, R.; Osgood, T.; Sun, J.-R.; Zhu, X.; McCarter, J. D.; Volak, L. P.; Houk, B. E.; Fakih, M. G.; O'Neil, B. H.; Price, T. J.; Falchook, G. S.; Desai, J.; Kuo, J.; Govindan, R.; Hong, D. S.; Ouyang, W.; Henary, H.; Arvedson, T.; Cee, V. J.; Lipford, J. R. The Clinical KRAS(G12C) Inhibitor AMG 510

Drives Anti-Tumour Immunity. *Nature* **2019**, *575* (7781), 217–223. (b) Perreault, S.; Chandrasekhar, J.; Patel, L. Atropisomerism in Drug Discovery: A Medicinal Chemistry Perspective Inspired by Atropisomeric Class I PI3K Inhibitors. *Acc. Chem. Res*. **2022**, *55* (18), 2581–2593. (c) Tucci, F. C.; Hu, T.; Mesleh, M. F.; Bokser, A.; Allsopp, E.; Gross, T. D.; Guo, Z.; Zhu, Y.-F.; Struthers, R. S.; Ling, N.; Chen, C. Atropisomeric Property of 1-(2,6-Difluorobenzyl)-3-[(2R)-Amino-2-Phenethyl]-5-(2-Fluoro-3-Methoxyphenyl)-6-Methyluracil. *Chirality* **2005**, *17* (9), 559–564.

(4) (a) Dial, B. E.; Pellechia, P. J.; Smith, M. D.; Shimizu, K. D. Proton Grease: An Acid Accelerated Molecular Rotor. *J. Am. Chem. Soc*. **2012**, *134* (8), 3675–3678. (b) Wu, Y.; Wang, G.; Li, Q.; Xiang, J.; Jiang, H.; Wang, Y. Publisher Correction: A Multistage Rotational Speed Changing Molecular Rotor Regulated by pH and Metal Cations. *Nat. Commun*. **2018**, *9* (1), 2364.

(5) (a) Cheng, J. K.; Xiang, S.-H.; Li, S.; Ye, L.; Tan, B. Recent Advances in Catalytic Asymmetric Construction of Atropisomers. *Chem. Rev*. **2021**, *121* (8), 4805–4902. (b) Wang, Y.-B.; Tan, B. Construction of Axially Chiral Compounds via Asymmetric Organocatalysis. *Acc. Chem. Res*. **2018**, *51* (2), 534–547. (c) Rodríguez-Salamanca, P.; Fernández, R.; Hornillos, V.; Lassaletta, J. M. Asymmetric Synthesis of Axially Chiral C-N Atropisomers. *Chem. Eur. J*. **2022**, *28* (28), e202104442. (d) Xiao, X.; Chen, B.; Yao, Y.-P.; Zhou, H.-J.; Wang, X.; Wang, N.-Z.; Chen, F.-E. Construction of Non-Biaryl Atropisomeric Amide Scaffolds Bearing a C-N Axis via Enantioselective Catalysis. *Molecules* **2022**, *27* (19), 6583.

(6) (a) Sun, C.; Qi, X.; Min, X.-L.; Bai, X.-D.; Liu, P.; He, Y. Asymmetric Allylic Substitution-Isomerization to Axially Chiral Enamides via Hydrogen-Bonding Assisted Central-to-Axial Chirality Transfer. *Chem. Sci*. **2020**, *11* (37), 10119–10126. (b) Wang, Y.-B.; Zheng, S.-C.; Hu, Y.-M.; Tan, B. Brønsted Acid-Catalysed Enantioselective Construction of Axially Chiral Arylquinazolinones. *Nat. Commun*. 2017, *8* (1), 15489. (c) Chu, Y.; Wu, M.; Hu, F.; Zhou, P.; Cao, Z.; Hui, X.-P. N-Heterocyclic Carbene-Catalyzed Atroposelective Synthesis of Pyrrolo[3,4-b]Pyridines with Configurationally Stable C-N Axial Chirality. *Org. Lett*. **2022**, *24* (21), 3884–3889. (d) Wang, W.; Jiang, M.; Li, J.; Wang, F.; Li, X.-X.; Zhao, J.; Li, X. Intermolecular Buchwald-Hartwig Reactions for Enantioselective Synthesis of Diverse Atropisomers: Rerouting the C-N Forming Mechanism to Substrate Oxygen-Assisted Reductive Elimination. *J. Am. Chem. Soc*. **2024**, *146* (24), 16567–16580.

(7) (a) Tanaka, K.; Takeishi, K.; Noguchi, K. Enantioselective Synthesis of Axially Chiral Anilides through Rhodium-Catalyzed [2+2+2] Cycloaddition of 1,6-Diynes with Trimethylsilylynamides. *J. Am. Chem. Soc*. **2006**, *128* (14), 4586–4587. (b) Tanaka, K.; Takahashi, Y.; Suda, T.; Hirano, M. Synthesis of Enantioenriched N-Aryl-2-Pyridones with Chiral C-N Axes by Rhodium-Catalyzed [2+2+2] Cycloaddition of Alkynes with Isocyanates. *Synlett* **2008**, *2008* (11), 1724–1728. (c) Onodera, G.; Suto, M.; Takeuchi, R. Iridium-Catalyzed [2+2+2] Cycloaddition of α,ω-Diynes with Isocyanates. *J. Org. Chem*. **2012**, *77* (2), 908–920. (d) Augé, M.; Barbazanges, M.; Tran, A. T.; Simonneau, A.; Elley, P.; Amouri, H.; Aubert, C.; Fensterbank, L.; Gandon, V.; Malacria, M.; Moussa, J.; Ollivier, C. Atroposelective [2+2+2] Cycloadditions Catalyzed by a Rhodium(i)–Chiral Phosphate System. *Chem. Commun*. **2013**, *49* (71), 7833. (e) Augé, M.; Feraldi-Xypolia, A.; Barbazanges, M.; Aubert, C.; Fensterbank, L.; Gandon, V.; Kolodziej, E.; Ollivier, C. Double-Stereodifferentiation in Rhodium-Catalyzed [2 + 2 + 2] Cycloaddition: Chiral Ligand/Chiral Counterion Matched Pair. *Org. Lett*. **2015**, 17 (15), 3754–3757. (f) Liu, Z.-S.; Xie, P.-P.; Hua, Y.; Wu, C.; Ma, Y.; Chen, J.; Cheng, H.-G.; Hong, X.; Zhou, Q. An Axial-to-Axial Chirality Transfer Strategy for Atroposelective Construction of C–N Axial Chirality. *Chem* **2021**, *7* (7), 1917–1932. (g) Si, X.-J.; Yang, D.; Sun, M.-C.; Wei, D.; Song, M.-P.; Niu, J.-L. Atroposelective Isoquinolinone Synthesis through Cobalt-Catalysed C–H Activation and Annulation. *Nat. Synth*. **2022**, *1* (9), 709–718. (h) Wang, B.-J.; Xu, G.-X.; Huang, Z.-W.; Wu, X.; Hong, X.; Yao, Q.-J.; Shi, B.-F. Single-Step Synthesis of Atropisomers with Vicinal C-C and C-N Diaxes by Cobalt-Catalyzed Atroposelective C-H Annulation. *Angew. Chem. Int. Ed*. **2022**, *61* (39), e202208912. (i) Wang, X.; Si, X.-J.; Sun, Y.; Wei, Z.; Xu, M.; Yang, D.; Shi, L.; Song, M.-P.; Niu, J.-L. C–N Axially Chiral Heterobiaryl Isoquinolinone Skeletons Construction via Cobalt-Catalyzed Atroposelective C–H Activation/Annulation. *Org. Lett*. **2023**, *25* (34), 6240–6245. (j) Lin, Y.; von Münchow, T.; Ackermann, L. Cobaltaelectro-Catalyzed C–H Annulation with Allenes for Atropochiral and P-Stereogenic Compounds: Late-Stage Diversification and Continuous Flow Scale-Up. *ACS Catal*. **2023**, *13* (14), 9713–9723. (k) Wang, P.; Wu, H.; Zhang, X.-P.; Huang, G.; Crabtree, R. H.; Li, X. Sigma-Bond Metathesis as an Unusual Asymmetric Induction Step in Rhodium-Catalyzed Enantiodivergent Synthesis of C–N Axially Chiral Biaryls. *J. Am. Chem. Soc*. **2023**, *145* (15), 8417–8429 (l) von Münchow, T.; Liu, Y.-R.; Parmar, R.; Peters, S. E.; Trienes, S.; Ackermann, L. Cobaltaelectro-Catalyzed C-H Activation for Central and Axial Double Enantio-Induction. *Angew. Chem. Int. Ed*. **2024**, *63* (31), e202405423. (m) Zhang, Y.; Liu, S.-L.; Li, T.; Xu, M.; Wang, Q.; Yang, D.; Song, M.-P.; Niu, J.-L. N,O-Auxiliary Enabled Cobaltaelectro-Catalyzed Atroposelective C–H Annulation. *ACS Catal*. **2024**, *14* (1), 1–9. (n) Xu, Y.; Lin, Y.; Homölle, S. L.; Oliveira, J. C. A.; Ackermann, L. Enantioselective Cobaltaphotoredox-Catalyzed C-H Activation. *J. Am. Chem. Soc*. **2024**, *146* (34), 24105–24113.

(8) (a) Kitagawa, O.; Kohriyama, M.; Taguchi, T. Catalytic Asymmetric Synthesis of Optically Active Atropisomeric Anilides through Enantioselective N-Allylation with Chiral Pd-Tol-BINAP Catalyst. *J. Org. Chem*. **2002**, *67* (24), 8682–8684. (b) Terauchi, J.; Curran, D. P. N-Allylation of Anilides with Chiral Palladium Catalysts: The First Catalytic Asymmetric Synthesis of Axially Chiral Anilides. *Tetrahedron Asymmetry* **2003**, *14* (5), 587–592. (c) Kitagawa, O.; Takahashi, M.; Yoshikawa, M.; Taguchi, T. Efficient Synthesis of Optically Active Atropisomeric Anilides through Catalytic Asymmetric N-Arylation Reaction *J. Am. Chem. Soc*. **2005**, *127* (18), 6910–6910. (d) Kitagawa, O.; Yoshikawa, M.; Tanabe, H.; Morita, T.; Takahashi, M.; Dobashi, Y.; Taguchi, T. Highly Enantioselective Synthesis of Atropisomeric Anilide Derivatives through Catalytic Asymmetric N-Arylation: Conformational Analysis and Application to Asymmetric Enolate Chemistry. *J. Am. Chem. Soc*. **2006**, *128* (39), 12923–12931. (e) Shirakawa, S.; Liu, K.; Maruoka, K. Catalytic Asymmetric Synthesis of Axially Chiral O-Iodoanilides by Phase-Transfer Catalyzed Alkylations. *J. Am. Chem. Soc*. **2012**, *134* (2), 916–919. (f) Li, S.-L.; Yang, C.; Wu, Q.; Zheng, H.-L.; Li, X.; Cheng, J.-P. Atroposelective Catalytic Asymmetric Allylic Alkylation Reaction for Axially Chiral Anilides with Achiral Morita-Baylis-Hillman Carbonates. *J. Am. Chem. Soc*. **2018**, *140* (40), 12836–12843. (g) Fan, X.; Zhang, X.; Li, C.; Gu, Z. Enantioselective Atropisomeric Anilides Synthesis via Cu-Catalyzed Intramolecular Adjacent C–N Coupling. *ACS Catal*. **2019**, *9* (3), 2286–2291. (h) Jin, L.; Li, Y.; Mao, Y.; He, X.-B.; Lu, Z.; Zhang, Q.; Shi, B.-F. Chiral Dinitrogen Ligand Enabled Asymmetric Pd/Norbornene Cooperative Catalysis toward the Assembly of C-N Axially Chiral Scaffolds. *Nat. Commun*. **2024**, *15* (1), 4908. (i) Arunachalampillai, A.; Chandrappa, P.; Cherney, A.; Crockett, R.; Doerfler, J.; Johnson, G.; Kommuri, V. C.; Kyad, A.; McManus, J.; Murray, J.; Myren, T.; Fine Nathel, N.; Ndukwe, I.; Ortiz, A.; Reed, M.; Rui, H.; Silva Elipe, M. V.; Tedrow, J.; Wells, S.; Yacoob, S.; Yamamoto, K. Atroposelective Brønsted Acid-Catalyzed Photocyclization to Access Chiral N-Aryl Quinolones with Low Rotational Barriers. *Org. Lett*. **2023**, *25* (31), 5856–5861. (j) Li, T.; Zhang, Y.; Du, C.; Yang, D.; Song, M.-P.; Niu, J.-L. Simultaneous Construction of Inherent and Axial Chirality by Cobalt-Catalyzed Enantioselective C-H Activation of Calix[4]Arenes. *Nat. Commun*. **2024**, *15* (1), 7673. (k) Qian, C.; Huang, J.; Huang, T.; Song, L.; Sun, J.; Li, P. Organocatalytic enantioselective synthesis of Csp^2–N atropisomers via formal Csp^2 –O bond amination. *Chem. Sci*., **2024**,15, 3893-3900.

(9) (a) Yao, Q.-J.; Xie, P.-P.; Wu, Y.-J.; Feng, Y.-L.; Teng, M.-Y.; Hong, X.; Shi, B.-F. Enantioselective Synthesis of Atropisomeric Anilides via Pd(II)-Catalyzed Asymmetric C-H Olefination. *J. Am. Chem. Soc*. **2020**, *142* (42), 18266–18276. (b) Li, H.; Yan, X.; Zhang, J.; Guo, W.; Jiang, J.; Wang, J. Enantioselective Synthesis of C-N Axially Chiral N-Aryloxindoles by Asymmetric Rhodium-Catalyzed Dual C-H Activation. *Angew. Chem. Int. Ed*. **2019**, *58* (20), 6732–6736.

(10) (a) Hata, T.; Koide, H.; Taniguchi, N.; Uemura, M. Asymmetric Synthesis of Axially Chiral Anilides by Enantiotopic Lithiation of Tri-

carbonyl(N-Methyl-N-Acyl-2,6-Dimethylanilide)Chromium Complex. *Org. Lett*. **2000**, *2* (13), 1907–1910. (b) Koide, H.; Hata, T.; Uemura, M. Asymmetric Synthesis of Axially Chiral Benzamides and Anilides by Enantiotopic Lithiation of Prochiral Arene Chromium Complexes. *J. Org. Chem*. **2002**, *67* (6), 1929–1935. (c) Yang, B.; Yang, J.; Zhang, J. Synthesis of Axially Chiral Anilides Enabled by a Palladium/Ming-Phos-Catalyzed Desymmetric Sonogashira Reaction. *Chin. J. Chem*. **2022**, 40 (3), 317–322. (d) Hirai, M.; Terada, S.; Yoshida, H.; Ebine, K.; Hirata, T.; Kitagawa, O. Catalytic Enantioselective Synthesis of N–C Axially Chiral Mebroqualone and Its Derivatives through Reductive Asymmetric Desymmetrization. *Org. Lett*. **2016**, 18, 21, 5700–5703. (e) Yoon, H.; Galls, A.; Rozema, S.D.; Miller, S.J. Atroposelective Desymmetrization of Resorcinol-Bearing Quinazolinones via Cu-Catalyzed C−O Bond Formation. *Org. Lett.* **2022** *24* (2), 762-766.

(11) (a) Motaleb, A.; Bera, A.; Maity, P. An Organocatalyst Bound α-Aminoalkyl Radical Intermediate for Controlled Aerobic Oxidation of Iminium Ions. *Org. Biomol. Chem*. **2018**, *16* (28), 5081–5085. (b) Baral, N.; Rani, S.; Saikia, P.; Maity, P. Organophosphites: An Addition to the Arsenal of Organocatalysts. *Eur. J. Org. Chem*. **2023**, *26*, e202201238.

(12) (a) Viana, G. H. R.; Santos, I. C.; Alves, R. B.; Gil, L.; Marazano, C.; Gil, R. P. F. Microwave-Promoted Synthesis of Chiral Pyridinium Salts. *Tetrahedron Lett*. **2005**, *46* (45), 7773–7776. (b) Zeghbib, N.; Thelliere, P.; Rivard, M.; Martens, T. Microwaves and Aqueous Solvents Promote the Reaction of Poorly Nucleophilic Anilines with a Zincke Salt. *J. Org. Chem*. **2016**, *81* (8), 3256–3262.

(13) (a) Tajuddeen, N.; Bringmann, G. N,C-Coupled Naphthylisoquinoline Alkaloids: A Versatile New Class of Axially Chiral Natural Products. *Nat. Prod. Rep*. **2021**, *38* (12), 2154–2186. (b) Bringmann, G.; Kajahn, I.; Reichert, M.; Pedersen, S. E. H.; Faber, J. H.; Gulder, T.; Brun, R.; Christensen, S. B.; Ponte-Sucre, A.; Moll, H.; Heubl, G.; Mudogo, V. Ancistrocladinium A and B, the First N,C-Coupled Naphthyldihydroisoquinoline Alkaloids, from a Congolese Ancistrocladus Species. *J. Org. Chem*. **2006**, *71* (25), 9348–9356. (c) Bringmann, G.; Gulder, T.; Hertlein, B.; Hemberger, Y.; Meyer, F. Total Synthesis of the N,C-Coupled Naphthylisoquinoline Alkaloids Ancistrocladinium A and B and Related Analogues. *J. Am. Chem. Soc*. **2010**, *132* (3), 1151–1158.

(14) Steinreiber, J.; Faber, K.; Griengl, H. De-Racemization of Enantiomers versus de-Epimerization of Diastereomers--Classification of Dynamic Kinetic Asymmetric Transformations (DYKAT). *Chem. Eur. J*. **2008**, *14* (27), 8060–8072.

(15) (a) Srivastava, V.; Singh, P. K.; Singh, P. P. Eosin Y Catalysed Visible-Light Mediated Aerobic Oxidation of Tertiary Amines. *Tetrahedron Lett*. **2019**, *60* (37), 151041. (b) Zhang, Y.; Riemer, D.; Schilling, W.; Kollmann, J.; Das, S. Visible-Light-Mediated Efficient Metal-Free Catalyst for α-Oxygenation of Tertiary Amines to Amides. *ACS Catal*. **2018**, *8* (7), 6659–6664.

(16) Jin, Y.; Ou, L.; Yang, H.; Fu, H. Visible-Light-Mediated Aerobic Oxidation of N-Alkylpyridinium Salts under Organic Photocatalysis. *J. Am. Chem. Soc*. **2017**, *139* (40), 14237–14243.

(17) Waldeck, D. H. Photoisomerization Dynamics of Stilbenes. *Chem. Rev*. **1991**, 91 (3), 415–436.

(18) Ong, J.-Y.; Ng, X. Q.; Lu, S.; Zhao, Y. Isothiourea-Catalyzed Atroposelective N-Acylation of Sulfonamides. *Org. Lett*. **2020**, *22* (16), 6447–6451.

(19) Asao, N.; Yudha S, S.; Nogami, T.; Yamamoto, Y. Direct Mannich and Nitro-Mannich Reactions with Non-Activated Imines: AgOTf-Catalyzed Addition of Pronucleophiles to Ortho-Alkynylaryl Aldimines Leading to 1,2-Dihydroisoquinolines. *Angew. Chem. Int. Ed*. **2005**, *44* (34), 5526–5528.

(20) (a) Nugen, T. T. Traceless point-to-axial chirality exchange in the atropselective synthesis of biaryls/heterobiaryls. *Org. Biomol. Chem*. **2019**, 17, 6952–6963. (b) Motaleb, A.; Rani, S.; Das, T.; Gonnade, R. G.; Maity, P. Phosphite-Catalyzed C-H Allylation of Azaarenes via an Enantioselective [2,3]-Aza-Wittig Rearrangement. *Angew. Chem. Int. Ed*. **2019**, *58* (40), 14104–14109.

(21) (a) Hari, D. P.; König, B. Synthetic Applications of Eosin Y in Photoredox Catalysis. Chem. Commun. (Camb.) 2014, 50, 6688–6699. (b) Bartling, H.; Eisenhofer, A.; König, B.; Gschwind, R. M. The Photocatalyzed Aza-Henry Reaction of N-Aryltetrahydroisoquinolines: Comprehensive Mechanism, $H^{\bullet}$ - versus H^{+} - Abstraction, and Background Reactions. *J. Am. Chem. Soc*. 2016, 138 (36), 11860–11871.

(22) (a) Perdew, J. P.; Burke, K.; Ernzerhof, M. Generalized Gradient Approximation Made Simple. *Phys. Rev. Lett*. **1996**, *77* (18), 3865–3868. (b) Grimme, S.; Antony, J.; Ehrlich, S.; Krieg, H. A Consistent and Accurate Ab Initio Parametrization of Density Functional Dispersion Correction (DFT-D) for the 94 Elements H-Pu. *J. Chem. Phys*. **2010**, *132* (15), 154104. (c) Schäfer, A.; Huber, C.; Ahlrichs, R. Fully Optimized Contracted Gaussian Basis Sets of Triple Zeta Valence Quality for Atoms Li to Kr. *J. Chem. Phys*. **1994**, *100* (8), 5829–5835. (d) Furche, F.; Ahlrichs, R.; Hättig, C.; Klopper, W.; Sierka, M.; Weigend, F. Turbomole: Turbomole. *Wiley Interdiscip. Rev. Comput. Mol. Sci*. **2014**, *4* (2), 91–100.

(23) Kumarasamy, E.; Jesuraj, J. L.; Omlid, J. N.; Ugrinov, A.; Sivaguru, J. Light-Induced Enantiospecific 4π Ring Closure of Axially Chiral 2-Pyridones: Enthalpic and Entropic Effects Promoted by H-Bonding. *J. Am. Chem. Soc*. **2011**, *133* (43), 17106–17109.

(24) Poplata, S.; Tröster, A.; Zou, Y.-Q.; Bach, T. Recent Advances in the Synthesis of Cyclobutanes by Olefin [2 + 2] Photocycloaddition Reactions. *Chem. Rev*. **2016**, *116* (17), 9748–9815.

(25) (a) Narasaka, K.; Hayashi, Y.; Shimadzu, H.; Niihata, S. Asymmetric [2 + 2] Cycloaddition Reaction Catalyzed by a Chiral Titanium Reagent. *J. Am. Chem. Soc*. **1992**, *114* (23), 8869–8885. (b) Coote, S. C.; Bach, T. Enantioselective Intermolecular [2+2] Photocycloadditions of Isoquinolone Mediated by a Chiral Hydrogen-Bonding Template. *J. Am. Chem. Soc*. **2013**, *135* (40), 14948–14951. (c) Tröster, A.; Alonso, R.; Bauer, A.; Bach, T. Enantioselective Intermolecular [2 + 2] Photocycloaddition Reactions of 2(1H)-Quinolones Induced by Visible Light Irradiation. *J. Am. Chem. Soc*. **2016**, *138* (25), 7808–7811.

(26) Al-Jalal, N.; Covell, C.; Gilbert, A. The Regio- and Stereo-Chemistries of the (2π+2π) Photocycloaddition of Electron-Deficient Ethenes to Isoquinolin-1(2H)-One. *J. Chem. Res. Synop*. **1998**, *11*, 678–678.

(27) (a) Lee-Ruff, E.; Mladenova, G. Enantiomerically Pure Cyclobutane Derivatives and Their Use in Organic Synthesis. *Chem. Rev*. **2003**, *103* (4), 1449–1483. (b) Wahl, M. H.; Jandl, C.; Bach, T. A [2 + 2] Photocycloaddition-Fragmentation Approach toward the Carbon Skeleton of Cis-Fused Lycorine-Type Alkaloids. *Org. Lett*. **2018**, *20* (23), 7674–7678.

(28) (a) Glorius, F.; Spielkamp, N.; Holle, S.; Goddard, R.; Lehmann, C. W. Efficient Asymmetric Hydrogenation of Pyridines. *Angew. Chem. Int. Ed.* **2004**, *43* (21), 2850–2852. (b) Wagener, T.; Lückemeier, L.; Daniliuc, C. G.; Glorius, F. Interrupted Pyridine Hydrogenation: Asymmetric Synthesis of δ-Lactams. *Angew. Chem. Int. Ed*. **2021**, *60* (12), 6425–6429.

(29) Gnecco, D.; Marazano, C.; Enríquez, R. G.; Terán, J. L.; Sánchez S, M. del R.; Galindo, A. Oxidation of Chiral Non-Racemic Pyridinium Salts to Enantiopure 2-Pyridone and 3-Alkyl-2-Pyridones. *Tetrahedron Asymmetry* **1998**, *9* (12), 2027–2029.